MDPI

Article

Deep Eutectic Solvents for the Separation of Toluene/1-Hexene via Liquid–Liquid Extraction

Mohamed K. Hadj-Kali [1],*, Lahssen El Blidi [1], Sarwono Mulyono [1], Irfan Wazeer [1], Emad Ali [1] and Jagan Rallapalli [2]

[1] Chemical Engineering Department, College of Engineering, King Saud University, Riyadh 11421, Saudi Arabia
[2] Functional Chemicals, Sabic Technology Centre, Riyadh 14334, Saudi Arabia
* Correspondence: mhadjkali@ksu.edu.sa

Abstract: The separation of aromatic/olefin mixtures is a difficult task in the petrochemical industry, since the boiling points of these hydrocarbons are very similar. This work aims to use deep eutectic solvents (DESs) for the extraction of toluene from 1-hexene by liquid–liquid extraction. A total of 53 DESs were studied qualitatively and quantitatively using the COSMO-RS approach to separate the binary mixture of toluene and 1-hexene. The selectivity, capacity, and performance index of all DESs were evaluated by calculating the activity coefficient at infinite dilution. The σ-profile and σ-potential of each component were interpreted to evaluate the interactions between the different species. We then selected three DESs for experimental validation, namely benzyltriphenylphosphonium chloride:triethylene glycol BzTPPCl:TEG (1:8), tetrabutylammonium bromide:triethylene glycol TBABr:TEG (1:3), and tetrabutylammonium bromide:ethylene glycol TBABr: EG (1:4). Experimental liquid–liquid equilibrium data were obtained for the ternary mixtures {1-hexene (1) + toluene (2) + DES (3)} at T = 298.15 K and atmospheric pressure. Based on the selectivity data and the solute distribution ratio, the feasibility of different DESs as extractive solvents was tested. Finally, ^{1}H NMR was performed to elucidate the extraction mechanism. No DES was found in the raffinate phase, indicating minimal cross-contamination.

Keywords: liquid–liquid extraction; deep eutectic solvents; COSMO-RS

1. Introduction

Aromatics produced by naphtha reforming and catalytic cracking are important feedstocks for many petrochemical applications [1]. Nevertheless, olefin impurities are common in aromatic streams. Therefore, it is necessary to separate aromatics and olefins. For such separation, three techniques are commercially used depending on the solution concentration: (i) at low aromatic content (20~65 wt%), liquid–liquid extraction is usually used; (ii) at medium aromatic content (65 to 90 wt%), extractive distillation is usually used; and (iii) at high aromatic content (>90 wt%), azeotropic distillation is used. However, to date, there is no practical process for separation when the aromatic content in the feed mixture is less than 20 wt%, while liquid extraction is considered the most favorable process when the aromatic content is less than 20%.

The process of separating the components of a liquid stream by contacting that stream with another liquid stream, which may be insoluble or only partially soluble, is called liquid–liquid extraction. It is possible to separate the components because some of them have a preference to be more soluble in one of the liquid streams than in the others. According to Coquelet and Ramjugernath [2], there are typically three distinct types of liquid–liquid equilibrium phase diagrams: (i) a binary component pair is partially miscible (type 1), (ii) two binary component pairs are somewhat miscible (type 2), and (iii) all three binary component pairs are somewhat miscible (type 3).

A critical step in the liquid–liquid extraction process is to find an efficient and cost-effective solvent. An ideal solvent should provide high extraction performance characterized by high solute selectivity, a high partition ratio, ease of regeneration, and a minimal feedstock to solvent ratio. From an environmental perspective, the solvent should also be environmentally friendly and non-toxic. From an economic point of view, the solvent should be available at low cost or should be able to be produced by a simple and cheap synthesis process. In addition, the physical and thermodynamic properties of the solvent, such as viscosity, thermal stability, density, and surface tension, are among the required information for industrial-scale applications. Traditional industrial-scale processes usually use organic solvents such as sulfolane (SUL), furfuryl alcohol, ethylene glycols, N-methylpyrrolidone and N-formylmorpholine.

However, the organic solvents have undesirable properties such as high toxicity, flammability, volatility and high cost of regeneration. Later, ionic liquid (IL) was introduced as a new advanced solvent and was extensively studied by researchers due to its invaluable advantage of negligible vapor pressure. To the best of our knowledge, the separation of toluene/1-hexene was described only by Meindersma et al. [3] using 3-methyl-N-butyl-pyridinium dicyanamide ([3-mebupy]N(CN)$_2$) IL in a pilot plant with rotating disk contactor at T = 303.15 K. The selectivity obtained was also reported. The selectivity obtained ranged from 5 to 13, while the distribution ratio for toluene ranged from 0.258 to 0.350 [3]. This result suggests that the IL has a higher affinity for toluene than for 1-hexene. This finding was also observed in aromatics/aliphatics separation, where the solvent tends to extract the aromatic compounds rather than the aliphatic ones [4–6]. Even more interestingly, the tie lines reported were identical to those determined for toluene-heptane. Consequently, we can assume that most of the solvents used for the separation of toluene/heptane could also be used for the separation of toluene and 1-hexene.

However, despite the clear advantages of ILs, most are too expensive to be used at an industrial scale. They are also more difficult to synthesize than organic solvents and are not consistently environmentally friendly [7,8]. To overcome the limitations of ILs, deep eutectic solvents (DESs) have been explored as versatile substitutes for ILs and organic solvents. A DES usually consists of two or more components that combine through hydrogen bonds to form eutectic mixtures and are characterized by a melting point lower than that of the individual components. The components of DES are commonly referred to as hydrogen bond donor (HBD) and hydrogen bond acceptor (HBA). DESs represent an evolving class of green solvents. Most of them have negligible vapor pressure [9], are biodegradable [10], biocompatible, non-flammable, and non- or low-toxic [11]. Several researchers have reported the use of different DESs for the separation of aromatic and aliphatic compounds [12,13] (Table S1).

Kareem et al. [14] used ETPI:SU and ETPI:EG DESs for the removal of toluene from heptane. However, it was found that EG or SU did not appear in the raffinate phase, indicating a critical problem in the removal of aromatics by liquid–liquid extraction. Wang et al. [5] studied the effect of HBAs on the extraction of toluene. The DESs with bromide-based quaternary ammonium salts showed higher values in selectivity and the distribution ratio than those based on chloride. Hou et al. [6] used tetrabutylphosphonium bromide (TBPBr) and tetrabutylammonium bromide (TBABr) as HBAs. The extraction rates of toluene for TBABr- and TBPBr-based DESs showed similar capacities, but TBPBr provided much higher selectivity than TBABr. In addition to HBAs, HBDs could also have a significant effect on extraction performance. Polyalcohols such as EG and TEG and carbonyl groups with carboxylic acid such as levulinic acid (LA) showed higher selectivities than sulfolane. Compared to EG, LA showed higher extraction efficiency, which was due to higher selectivity of toluene. This could be due to the fact that the carbon-oxygen double bond (C=O) present in the structure of LA could enhance its interaction with the aromatic ring of toluene by forming a π–π bond.

Numerous thermodynamic predictions and validations in critical steps such as denitrification [15], desulfurization [16,17], and separation of aromatic and aliphatic mixtures [18–20]

have been performed using the Conductor-like Screening Model for Realistic Solvents (COSMO-RS). In this study, COSMO-RS screening and experimental liquid–liquid extraction were used to investigate and validate the extraction performance of DESs for the separation of toluene from 1-hexene.

2. COSMO-RS Screening

In the initial phase of this work, we performed a literature search and proposed more than 100 potential DESs for the separation of toluene from 1-hexene. These DESs were successfully synthesized, characterized, and used in many applications reported in the literature. They were mainly ammonium-, phosphonium-, and choline-based DESs with a variety of HBDs. However, when searching the database COSMO-RS provided by the supplier, it was found that some components of these DESs were not available. To address this issue, the molecular geometry of the unavailable compounds was calculated using the TurboMole program package, also provided by the same vendor. Geometry optimization of these compounds was successfully performed. Nevertheless, some compounds were omitted due to their polymer nature (PEG 200, PEG 400, PEG 600, PEG 1000, and PEG 4000) and the inability to import ".*cosmo*" files into COSMOtherm (betaine, betaine hydrochloride, caffeic acid, choline acetyl chloride, p-toluenesulfonic acid, and trimethyl hydrochloride). These restrictions brought the DES candidates to a shortlist of 53 types (Table 1) that were finally included in the COSMO-RS screening.

Table 1. List of the shortlisted DESs for COSMO-RS screening.

No.	HBA	HBD	Abbreviation
1	Benzyltriphenylphosphonium chloride	Triethylene glycol	BzTPPCl:TEG (1:8)
2	Tetrabutylammonium bromide	Triethylene glycol	TBABr:TEG (1:3)
3	Methyltriphenylphosponium bromide	Triethylene glycol	MTPPBr:TEG (1:4)
4	Tetrabutylammonium bromide	Levulinic acid	TBABr:LA (1:3)
5	Tetrabutylammonium bromide	Levulinic acid	TBABr:LA (1:2)
6	Methyltriphenylphosponium bromide	Levulinic acid	MTPPBr:LA (1:4)
7	Tetrabutylammonium bromide	Ethylene glycol	TBABr:EG (1:2)
8	Tetrabutylphosphonium bromide	Ethylene glycol	TBPBr:EG (1:2)
9	Tetraethylammonium bromide	Levulinic acid	TEABr:LA (1:3)
10	Methyltriphenylphosponium bromide	Ethylene glycol	MTPPBr:EG (1:5)
11	Choline chloride	Triethylene glycol	ChC:TEG (1:3)
12	Choline chloride	Tartaric acid	ChCl:TA (2:1)
13	Choline chloride	1,4-Butanediol	ChCl:1,4-BD (1:4)
14	Tetrabutylammonium chloride	Malonic acid	TBACl:MalA (1:3)
15	Benzyltrimethylammonium chloride	Levulinic acid	BzTMACl:LA (1:4)
16	Tetraethylammonium chloride	Glycerol	TEACl:Gly (1:2)
17	Caprolactam	imidazole	Capr:Im (1:1)
18	1-ethyl-3-methylimidazolium chloride	Ethylene glycol	EmimCl:EG (1:2)
19	Caprolactam	acetamide	Capr:Act (1:1)
20	Choline chloride	Phenol	ChCl:Phe (1:4)
21	Tetramethylammonium chloride	Ethylene glycol	TMACl:EG (1:3)
22	Choline chloride	1,2-Propanediol	ChCl:PD (1:4)
23	L-carnitine	Phenol	Carn:Phe (1:3)
24	Choline chloride	Levulinic acid	ChCl:LA (1:3)
25	Choline chloride	Diethylene glycol	ChCl:DEG (1:2)
26	Choline chloride	1,4-Butanediol	ChCl:1,4-BD (1:2)
27	Choline chloride	1,3-Butanediol	ChCl:1,3-BD (1:2)
28	Choline chloride	1,6-Hexanediol	ChCl:1,6-HD (1:2)
29	Choline chloride	Phenylpropionic acid	ChCl:PhPA (1:2)
30	Choline chloride	Ethylene glycol	ChCl:EG (1:2)
31	Tetramethylammonium chloride	Glycerol	TMACl:Gly (1:2)
32	Choline chloride	Acetic acid	ChCl:AcA (1:2)
33	Choline chloride	2,3-Butanediol	ChCl:2,3-BD (1:2)

Table 1. *Cont.*

No.	HBA	HBD	Abbreviation
34	Choline chloride	Levulinic acid	ChCl:LA (1:2)
35	Tetramethylammonium chloride	Glycerol	TMACl:Gly (1:5)
36	Tetramethylammonium chloride	Phenylacetic acid	TMACl:PAA (1:2)
37	Choline chloride	1,2-Butanediol	ChCl:1,2-BD (1:2)
38	Tetramethylammonium chloride	Glycerol	TMACl:Gly (1:4)
39	Choline chloride	Phenylacetic acid	ChCl:PhAA (1:2)
40	Choline chloride	Benzoic acid	ChCl:BzA (1:2)
41	Choline chloride	Glycerol	ChCl:Gly (1:4)
42	Choline chloride	Urea	ChCl:Ur (1:2)
43	Choline chloride	Xylitol	ChCl:Xy (1:1)
44	Choline chloride	Glycerol	ChCl:Gly (1:2)
45	Choline chloride	Malonic acid	ChCl:MalA (1:1)
46	Choline chloride	D-sorbitol	ChCl:Sorb (1:1)
47	Choline chloride	Malic acid	ChCl:MA (1:1)
48	Choline chloride	Oxalic acid	ChCl:OA (1:1)
49	Choline bromide	Urea	ChBr:Ur (1:2)
50	Choline chloride	Citric acid	ChCl:CA (1:1)
51	Choline chloride	Glycolic acid	ChCl:GA (1:3)
52	Chlorocholine chloride	Urea	ClChCl:Ur (1:2)
53	Choline chloride	Thiourea	ChCl:Tur (1:2)

Screening Methodology

Geometry optimization of species not available in the database COSMO-RS was performed using the program package Turbomole (TmoleX). In this program, the chemical structure of the target molecule was first drawn. Then, geometry optimization was performed at the Hartree–Fock level and the 6-31G* basis set. To use COSMO-RS as a screening tool, you need to create the *".cosmo"* files of the target components (salt cations, salt anions, and HBDs). The *".cosmo"* file of a molecule contains information about the screening charge density (σ) of the segmented molecule in a virtual conductor environment. The *".cosmo"* file was generated by a one-point calculation using density functional theory (DFT) with Becke–Perdew and the triple-ζ zeta valence potential (TZVP) basis set. Finally, the *".cosmo"* files were exported to the COSMOthermX program with the parameterization BP _TZVP_C30_1301.ctd.

The activity coefficient at infinite dilution (γ^∞) of toluene and 1-hexene in each DES was predicted using the generated *".cosmo"* files in the COSMO-RS calculations. The selectivity of a DES to the solute compared to the carrier ($S^\infty_{Toluene,1-hexene}$) can be expressed by the ratio of the activity coefficient for carrier and solute (Equation (1)).

$$S^\infty_{Toluene,1-hexene} = \frac{\gamma^\infty_{1-hexene}}{\gamma^\infty_{Toluene}} \tag{1}$$

In addition, the capacity at infinite dilution (C^∞) can be used to qualitatively determine the amount of a DES required for the extraction process. In this study, the capacity of a DES for solute ($C^\infty_{Toluene}$) indicates the maximum amount of solute that can be dissolved in the DES, and can be obtained by using the following equation:

$$C^\infty_{Toluene} = \frac{1}{\gamma^\infty_{Toluene}} \tag{2}$$

The final parameter used to evaluate solvent properties in this extraction procedure is the performance index at infinite dilution (PI^∞). In this process, the two characteristics of capacity and selectivity are combined to estimate the overall performance of a DES. PI is simply expressed as the product of selectivity and capacity.

$$PI^\infty = S^\infty_{Toluene,\ 1-hexene} \times C^\infty_{Toluene} \tag{3}$$

The performance of DESs for the separation of toluene and 1-hexene was compared using estimated C^∞ and S^∞ values. The BP_TZVPD_FINE_C30_1401.ctd parametrization file was used in the COSMOthermX program to perform the COSMO-RS calculations. DESs were represented using an electroneutral approach in the COSMO-RS approach as suggested by the developer of the COSMOtherm package for representing Ils. There are two other approaches that can be used in addition to the electroneutral approach to represent DESs in COSMO-RS, viz., metafile and ion-pair approaches. However, we chose the electroneutral approach because our previous studies have shown that it best describes the presence of Ils and DESs in the bulk mixture [21,22]. The COSMO-RS screening results with respect to C^∞ and S^∞ are shown in Figures 1 and 2, respectively, and PI^∞ is represented in Figure S1.

It is worth noting that the low C^∞ and S^∞ values were obtained in comparison to other systems in this work as well as in previous work with other aromatic-aliphatic separations [18,20,23,24]. This would support the extent of difficulty in separating 1-hexene and n-toluene. This would also necessitate experimental studies to validate the screening results, as the experimental results would reflect the actual extraction performance.

The COSMO-RS screening results in terms of capacity, selectivity, and the performance index at infinite dilution are reported in the supporting information (Table S2). Table 2 summarizes the top ten DESs from the COSMO-RS screening for each evaluation criteria (C^∞, S^∞, and PI^∞). It is noteworthy that TBABr:TEG (1:3) was not only highest for $S\infty$, but was also among the top performers for C^∞ DES. It is expected that the highest value of C^∞ produced with BzTPPCl:TEG (1:8) is due to the high content of triethylene glycol (TEG), which increases the interaction with both 1-hexene and toluene. The potential DESs for experimental validation based on capacity and selectivity are TBABr:TEG (1:3), BzTPPCl:TEG (1:8), and TBABr:EG (1:4). Sigma surfaces of the HBAs, HBDs, as well as the sigma profile and sigma potential of three selected DESs for the toluene-1-hexene system are included in the supporting information (Figures S2–S4). MTPPBr:TEG (1:4) was not selected because it had the lowest selectivity among the top ten DESs in the COSMO-RS screening. In addition, TBABr:LA (1:2) and TBABr:LA (1:3) were also rejected because levulinic acid appeared in the raffinate phase (Figure S5).
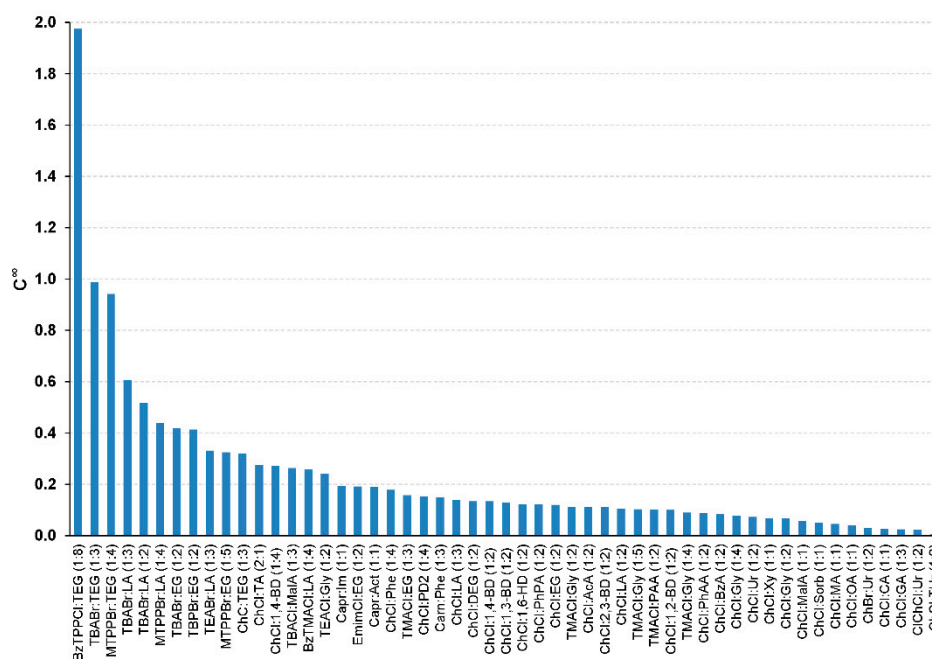

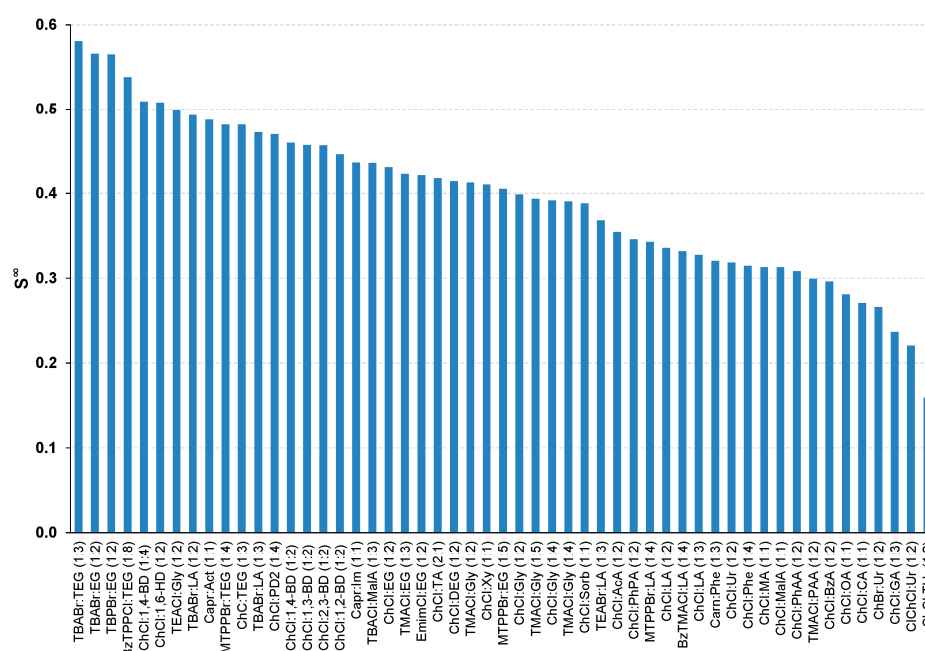**Figure 1.** Capacity of the selected DESs at infinite dilution.

Figure 2. Selectivity of the selected DESs at infinite dilution.

Table 2. The top 10 DESs according to COSMO-RS screening by C^∞, S^∞ and PI^∞ for the separation of 1-hexene and toluene.

No.	Capacity		Selectivity		Performance Index	
	DES	C^∞	**DES**	S^∞	**DES**	PI^∞
1	BzTPPCl:TEG (1:8)	1.975	TBABr:TEG (1:3)	0.580	BzTPPCl:TEG (1:8)	1.063
2	TBABr:TEG (1:3)	0.988	TBABr:EG (1:2)	0.566	TBABr:TEG (1:3)	0.573
3	MTPPBr:TEG (1:4)	0.941	TBPBr:EG (1:2)	0.565	MTPPBr:TEG (1:4)	0.453
4	TBABr:LA (1:3)	0.604	BzTPPCl:TEG (1:8)	0.538	TBABr:LA (1:3)	0.285
5	TBABr:LA (1:2)	0.515	ChCl:1,4-BD (1:4)	0.509	TBABr:LA (1:2)	0.254
6	MTPPBr:LA (1:4)	0.439	ChCl:1,6-HD (1:2)	0.508	TBABr:EG (1:2)	0.236
7	TBABr:EG (1:2)	0.418	TEACl:Gly (1:2)	0.498	TBPBr:EG (1:2)	0.233
8	TBPBr:EG (1:2)	0.412	TBABr:LA (1:2)	0.492	ChC:TEG (1:3)	0.154
9	TEABr:LA (1:3)	0.330	Capr:Act (1:1)	0.487	MTPPBr:LA (1:4)	0.150
10	MTPPBr:EG (1:5)	0.323	MTPPBr:TEG (1:4)	0.481	ChCl:1,4-BD (1:4)	0.138

Synthesis of these three potential candidates (BzTPPCl:TEG (1:8), TBABr:TEG (1:3), and TBABr:EG (1:4)) is then necessary to validate their actual performance. After they are successfully synthesized and characterized, the actual performance is determined in liquid–liquid extraction experiments. The liquid–liquid equilibria (LLE) data for each DES will be examined and supported with thermodynamic models and consistency tests.

3. Materials and Methods

The materials used for the extraction process are listed in Table 3, including purity, CAS number, and origin. For all compounds, purities refer to the mass fraction reported by the manufacturer. Each chemical was used directly without further purification.

Compound	Purity [a] (wt %)	CAS No.	Origin
Toluene	99.9 (GC) [b]	108-88-3	Scarlav (Spain)
1-hexene	97.0 (GC)	592-41-6	Aldrich (USA)
Benzyl triphenyl phosphonium chloride	99.0 (Argentometry)	1449-46-3	Acros Organics (England)
Tetrabutyl ammonium bromide	98.0 (Argentometry)	1643-19-2	Loba Chemie (India)
Ethylene glycol	99.0 (GC)	107-21-1	Winlab (England)
Triethylene glycol	99.0 (GC)	112-27-6	Acros Organics (USA)
Sulfolane	99.0 (GC)	126-33-0	Acros Organics (USA)

[a] The purities of chemicals are provided by the suppliers. [b] Gas chromatography.

3.1. DESs Synthesis and Physical Properties

The structures of the DESs studied are shown in Figure 3. Three different DESs, namely BzTPPCl:TEG (1:8) (DES #1), TBABr:TEG (1:3) (DES #2), and TBABr:EG (1:4) (DES #3), were synthesized according to the method described by Abbott et al. [25]. The different salts were mixed with HBD in various molar ratios in screw-capped bottles. The bottles were then placed in an incubator shaker at a rotation speed of 200 rpm and a temperature of 80 °C (±0.1 °C) until a clear liquid was formed.
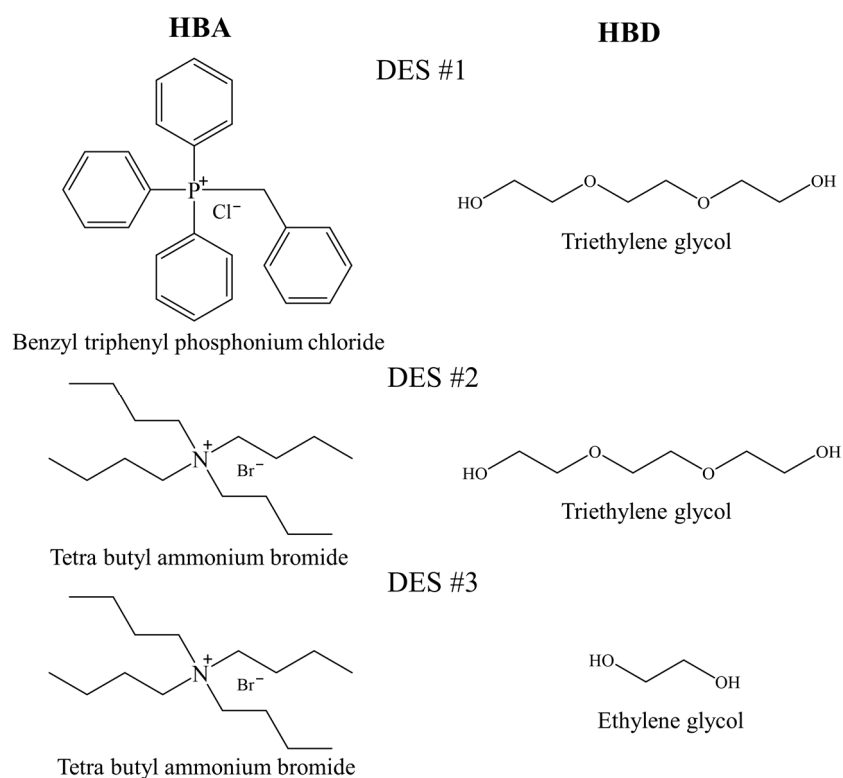

Figure 3. The structures of the DESs used in the experiment process.

Table 4 shows the physical properties (densities and viscosities) of prepared DESs. An Anton Paar DMA 4100 M densiometer with a repeatability and precision of 0.05 kg/m^3 and 0.1 kg/m^3, respectively, was used to measure the densities of DESs at 101.3 Kpa. The approach described in the literature [26] was used to determine the standard uncertainties of the densities considering the chemical purity. An Anton Paar Lovis 2000 M/ME viscometer set at 101.3 kPa and with a relative accuracy of 0.005 was used to measure the viscosities of the DESs. The falling ball concept is used to determine viscosity with the Lovis 2000 M/ME. The sample was placed in the Lovis 2000 M/ME to measure the falling time of the ball in a calibrated glass capillary with a steel ball as supplied by the manufacturer. The viscosities were calculated three times to obtain the average values, and the standard

uncertainties of the viscosities were calculated using the equation given below, assuming that the calculated values fell into a triangular probability distribution [27]:

$$u(\eta) = \frac{\eta_+ - \eta_-}{\sqrt{6}} \tag{4}$$

where η_+ and η_- are the upper and lower limits of the measured values.

Table 4. Densities (ρ) and viscosities (η) of the prepared DESs at temperature T = 298.15 K and pressure P = 101.3 kPa [a].

DES	Density (kg/m^3)	Viscosity (mPa·s)
BzTPPCl:TEG (1:8)	1141.3 ± 2.0	123.24 ± 1.30
TBABr:TEG (1:3)	1092.9 ± 2.0	121.60 ± 1.55
TBABr:EG (1:4)	1076.6 ± 2.0	68.72 ± 0.39

[a] Standard uncertainties are u(T) = 0.1 K, u(P) = 1 kPa, u(η) and u(ρ) are reported inside the table following the ±sign.

3.2. Extraction Procedure

An analytical balance (±0.0001 g) was used to prepare the feed mixture by mixing the weighed amounts of the materials. The feed was then mixed with the DESs at a mass ratio of 1:1. The flasks were placed in an incubator shaker and each series of experiments was performed at 298.15 K. Shaking was performed for 6 h followed by a settling period of ~12 h to ensure that thermodynamic equilibrium was reached. After intensive shaking and settling, two layers evidently appeared in the vials. Samples were then taken from both phases (upper and lower layers) and analyzed by gas chromatography (GC). Samples from both layers were diluted with diethyl ether.

We performed liquid–liquid equilibrium experiments for the separation of toluene from 1-hexene using DES 1, 2 and 3. The Trace GC ultra system (Thermo Scientific) consisted of a flame ionization detector (FID) and an Rtx-1 column (100% dimethylpolysiloxane, 30 m, 0.25 mmID, 0.25 μm df) used for characterization. Helium with a split mode was used as the carrier gas. A calibration curve of toluene/1-hexene was prepared to measure the composition (Figure S6). The optimal conditions of trace GC ultra for the toluene/1-hexene system are given in Table 5. We triplicated each experimental measurement, and the reported average uncertainty of the molar compositions was estimated to be ±0.007. The detailed discussion about the uncertainty calculations is presented in the Appendix A. To confirm the absence of DESs in the top layer, samples from this layer were analyzed by ^{1}H NMR spectroscopy using the JEOL RESONANCE spectrometer ECX-500 II). Dimethyl sulfoxide (DMSO-d6) was used as solvent for dilution and the ^{1}H NMR spectra were recorded at 297.15 K. In addition, the water content of the three different DESs was measured by Karl Fischer titration (Aquamax Karl-Fischer, GR Scientific Ltd., Halle, Germany). It was found that the water content for each DES was less than 1 wt% (water content for DES #1 = 0.048 wt%, DES #2 = 0.092 wt%, and DES #3 = 0.068 wt%).

Table 5. GC conditions for the toluene/1-hexene system.

Parameter	
Temperature of injector (K)	473.15
Temperature of detector (K)	553.15
Carrier gas pressure (Kpa)	100
Oven program	308.15 K for 2 min 308.15 K to 373.15 K Rate: 30 K/min Hold time: 0 min

4. Results and Discussion

4.1. Selectivity and the Distribution Ratio

Selectivity (S) and the distribution ratio (D) were used to evaluate the performance of the extraction process. The affinity of toluene for DES (as a solvent) can be determined by selectivity, which is defined as the ratio between the partition coefficient of the solute and the partition coefficient of the carrier (1-hexene) (see Equation (5) below). On the other hand, D is the ratio between the solute concentration in the extract layer and its concentration in the raffinate layer, as given in Equation (6).

$$S = \frac{D_{tol}}{D_{hex}} = \frac{\frac{w'_{tol}}{w''_{tol}}}{\frac{w'_{hex}}{w''_{hex}}} = \frac{w'_{tol}}{w''_{tol}} \times \frac{w''_{hex}}{w'_{hex}} \tag{5}$$

$$D_{tol} = \frac{w'_{tol}}{w''_{tol}} \tag{6}$$

In the above equations, w_{hex} is the concentration of 1-hexene in mole fraction, while w_{tol} is the concentration of toluene in mole fraction. The superscripts $'$ and $''$ denote the extract and raffinate layers, respectively.

The compositions of the extract and raffinate phases are given in Tables 6–8 using DES 1, 2, and 3, respectively, and are shown in Figure 4, which shows that all three DES were absent in the raffinate phase. This observation is confirmed by the ^{1}H NMR spectra of the raffinate phase in Figures S6–S8, which show that there is no peak representing DES components in the extract phase. The absence of DESs in the raffinate phase favored the solvent recovery. Figure 4 illustrates the phase behavior of the studied mixture {1-hexene + toluene + DES}. The studied aromatic compound (toluene) was completely miscible with 1-hexene and partially miscible with DESs. Therefore, all three phase diagrams demonstrated characteristics of type 2 behavior [2]. The extractability of three DESs with toluene/1-hexene compositions from 10 to 90 wt% in the feed was studied. The trend of D and S using three DESs is shown in Figures 5–7 as a function of 1-hexene composition in the feed.

Table 6. Composition of the experimental tie-lines (mole fraction), the toluene distribution ratio (D) and selectivity (S) for the ternary system {1-hexene (1) + toluene (2) + DES #1 (3)} at 298.15 K and 101.325 kPa [a].

Top Layer			Bottom Layer			D_{tol}	S
x_1	x_2	x_3	x_1	x_2	x_3		
0.923 ± 0.036	0.077 ± 0.003	0	0.068 ± 0.002	0.029 ± 0.001	0.903 ± 0.026	0.379 ± 0.005	5.18 ± 0.52
0.838 ± 0.032	0.162 ± 0.006	0	0.058 ± 0.002	0.059 ± 0.002	0.883 ± 0.025	0.368 ± 0.005	5.33 ± 0.51
0.739 ± 0.028	0.261 ± 0.010	0	0.045 ± 0.002	0.078 ± 0.003	0.877 ± 0.033	0.298 ± 0.006	4.86 ± 0.52
0.653 ± 0.025	0.347 ± 0.013	0	0.047 ± 0.002	0.120 ± 0.004	0.833 ± 0.032	0.346 ± 0.005	4.76 ± 0.51
0.568 ± 0.021	0.432 ± 0.016	0	0.052 ± 0.003	0.180 ± 0.007	0.768 ± 0.029	0.416 ± 0.007	4.55 ± 0.50
0.468 ± 0.018	0.532 ± 0.020	0	0.077 ± 0.002	0.232 ± 0.009	0.691 ± 0.026	0.436 ± 0.012	2.66 ± 0.28
0.362 ± 0.014	0.638 ± 0.024	0	0.057 ± 0.002	0.256 ± 0.010	0.687 ± 0.026	0.402 ± 0.012	2.55 ± 0.28
0.244 ± 0.009	0.756 ± 0.029	0	0.048 ± 0.002	0.305 ± 0.012	0.647 ± 0.025	0.403 ± 0.015	2.04 ± 0.22
0.125 ± 0.005	0.875 ± 0.035	0	0.033 ± 0.001	0.407 ± 0.016	0.561 ± 0.022	0.465 ± 0.021	1.78 ± 0.20

[a] Standard uncertainties are u(x) = 0.010, u(T) = 0.5 K and u(P) = 1.0 kPa.

Table 7. Composition of the experimental tie-lines (mole fraction), the toluene distribution ratio (D) and selectivity (S) for the ternary system {1-hexene (1) + toluene (2) + DES #2 (3)} at 298.15 K and 101.325 kPa [a].

| Top Layer			Bottom Layer			D_{tol}	S
x_1	x_2	x_3	x_1	x_2	x_3		
0.915 ± 0.036	0.085 ± 0.003	0	0.022 ± 0.002	0.010 ± 0.001	0.968 ± 0.025	0.115 ± 0.002	4.68 ± 0.45
0.823 ± 0.032	0.177 ± 0.007	0	0.017 ± 0.002	0.022 ± 0.002	0.961 ± 0.024	0.133 ± 0.002	4.81 ± 0.46
0.728 ± 0.028	0.272 ± 0.010	0	0.031 ± 0.003	0.053 ± 0.005	0.916 ± 0.027	0.195 ± 0.003	4.60 ± 0.49
0.634 ± 0.024	0.366 ± 0.014	0	0.025 ± 0.003	0.070 ± 0.007	0.905 ± 0.026	0.191 ± 0.003	4.77 ± 0.51
0.551 ± 0.021	0.449 ± 0.017	0	0.036 ± 0.004	0.141 ± 0.010	0.823 ± 0.020	0.313 ± 0.005	4.74 ± 0.51
0.468 ± 0.018	0.532 ± 0.020	0	0.043 ± 0.004	0.218 ± 0.014	0.739 ± 0.016	0.409 ± 0.007	4.45 ± 0.48
0.365 ± 0.014	0.635 ± 0.024	0	0.040 ± 0.003	0.265 ± 0.020	0.695 ± 0.015	0.418 ± 0.008	3.85 ± 0.41
0.257 ± 0.010	0.743 ± 0.028	0	0.029 ± 0.002	0.319 ± 0.024	0.652 ± 0.012	0.429 ± 0.009	3.80 ± 0.41
0.125 ± 0.005	0.875 ± 0.034	0	0.034 ± 0.002	0.427 ± 0.028	0.539 ± 0.009	0.488 ± 0.022	1.78 ± 0.20

[a] Standard uncertainties are u(x) = 0.008, u(T) = 0.5 K and u(P) = 1.0 kPa.

Table 8. Composition of the experimental tie-lines (mole fraction), the toluene distribution ratio (D) and selectivity (S) for the ternary system {1-hexene (1) + toluene (2) + DES #3 (3)} at 298.15 K and 101.325 kPa [a].

Top Layer			Bottom Layer			D_{tol}	S
x_1	x_2	x_3	x_1	x_2	x_3		
0.927 ± 0.036	0.073 ± 0.02	0	0.073 ± 0.003	0.030 ± 0.001	0.897 ± 0.024	0.408 ± 0.039	5.13 ± 0.50
0.842 ± 0.032	0.158 ± 0.006	0	0.069 ± 0.002	0.058 ± 0.002	0.873 ± 0.023	0.369 ± 0.032	4.50 ± 0.43
0.742 ± 0.028	0.258 ± 0.009	0	0.046 ± 0.004	0.061 ± 0.004	0.893 ± 0.031	0.237 ± 0.029	3.79 ± 0.41
0.642 ± 0.024	0.358 ± 0.014	0	0.037 ± 0.002	0.070 ± 0.004	0.893 ± 0.032	0.196 ± 0.022	3.45 ± 0.38
0.541 ± 0.020	0.459 ± 0.018	0	0.033 ± 0.002	0.083 ± 0.005	0.884 ± 0.031	0.182 ± 0.021	3.01 ± 0.33
0.454 ± 0.017	0.546 ± 0.021	0	0.037 ± 0.002	0.126 ± 0.008	0.837 ± 0.028	0.231 ± 0.027	2.80 ± 0.30
0.353 ± 0.013	0.647 ± 0.025	0	0.036 ± 0.002	0.162 ± 0.009	0.802 ± 0.027	0.250 ± 0.028	2.47 ± 0.27
0.241 ± 0.009	0.759 ± 0.029	0	0.023 ± 0.001	0.193 ± 0.010	0.784 ± 0.027	0.254 ± 0.027	2.65 ± 0.29
0.126 ± 0.005	0.874 ± 0.035	0	0.015 ± 0.001	0.251 ± 0.015	0.734 ± 0.024	0.287 ± 0.035	2.33 ± 0.26

[a] Standard uncertainties are u(x) = 0.004, u(T) = 0.5 K and u(P) = 1.0 kPa.

Among the HBD, TEG had the highest performance index (PI). The longer chain of TEG could be a justification for this PI compared to other HBDs, which allowed better affinity to 1-hexene due to the interactions between the alkene double bond and the hydroxyl group of TEG and the interactions between the hydrophobic part of the alkene and the methylene groups of TEG. The results proved that the three DESs have similar performance. Each sample was analyzed at least three times and the average was reported in Tables 6–8. The uncertainty calculations for the separation of toluene and 1-hexene using the three DESs can be found in the supporting information. Figures 5–7 show the variation of the distribution ratio and selectivity for the separation of 1-hexeneand toluene using three different DESs at 298.15 K and 101.325 kPa.
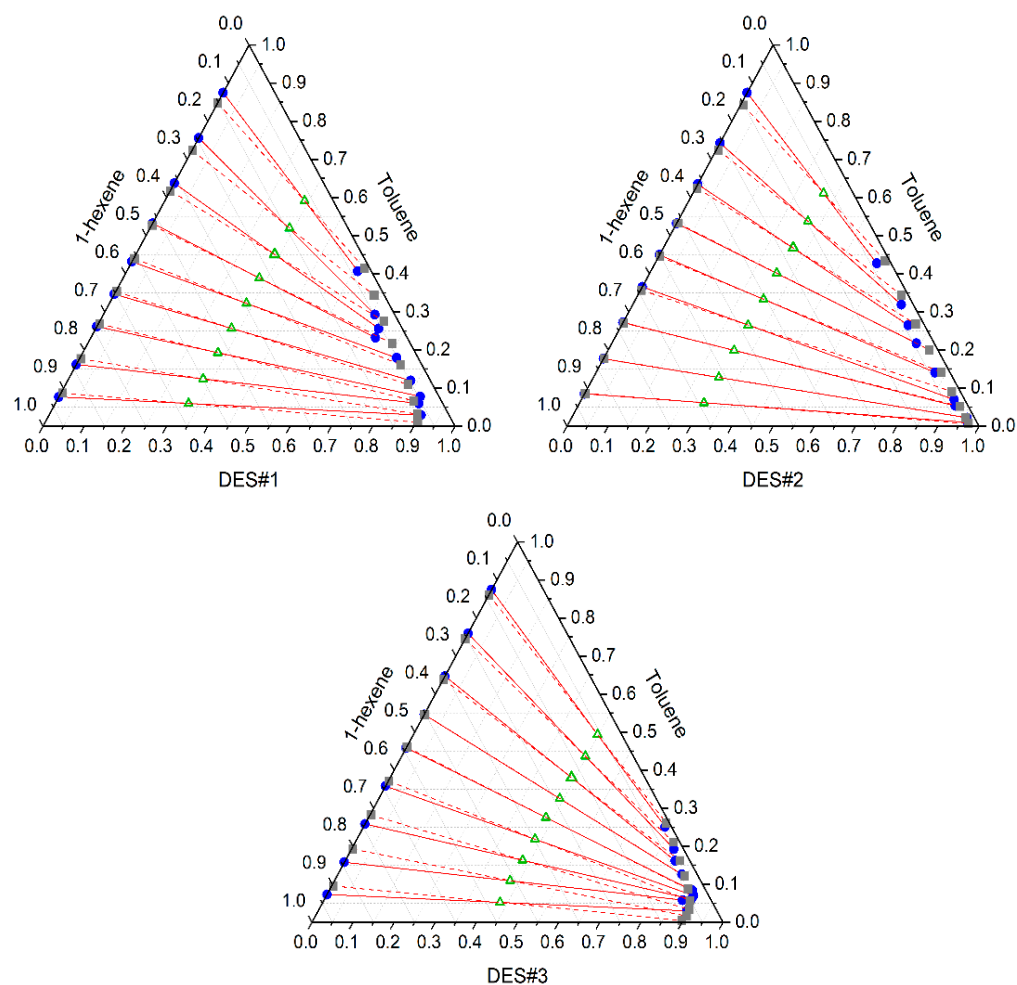
Figure 4. Liquid–liquid equilibrium diagram for the ternary systems {1-hexene (1) + toluene (2) + DES (3)} at T = 298.15 K and atmospheric pressure. Experimental data (● —); NRTL model (■ – –).
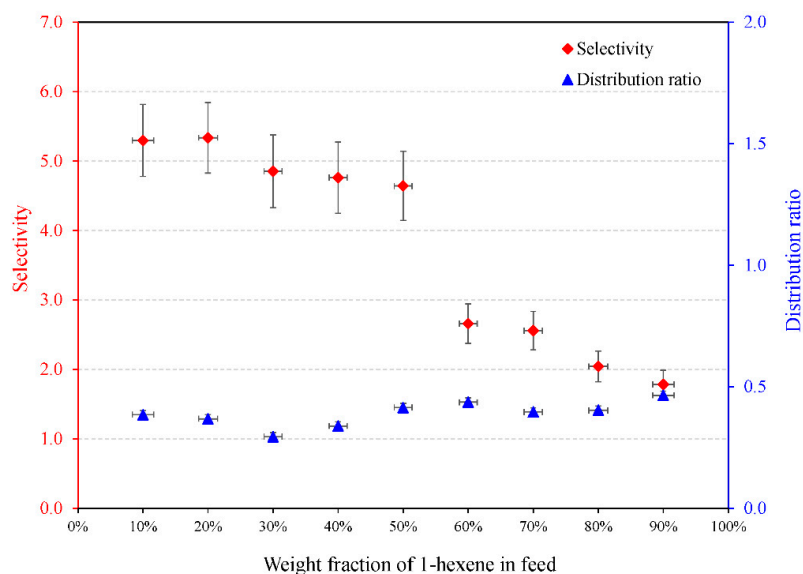
Figure 5. Variation of the selectivity and the distribution ratio with toluene weight fraction in the feed for {1-hexene (1) + toluene (2) + DES #1 (3)}.
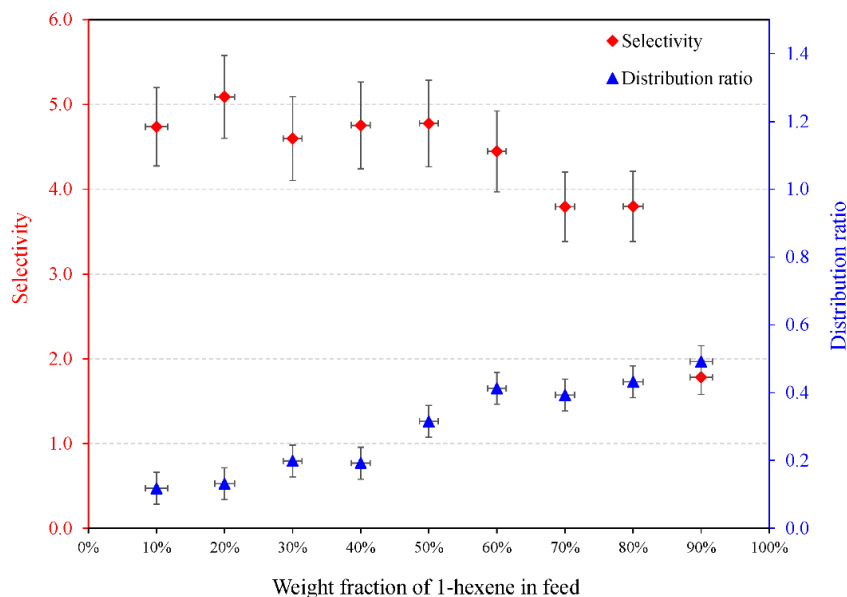
Figure 6. Variation of the selectivity and the distribution ratio with toluene weight fraction in the feed for {1-hexene (1) + toluene (2) + DES #2 (3)}.
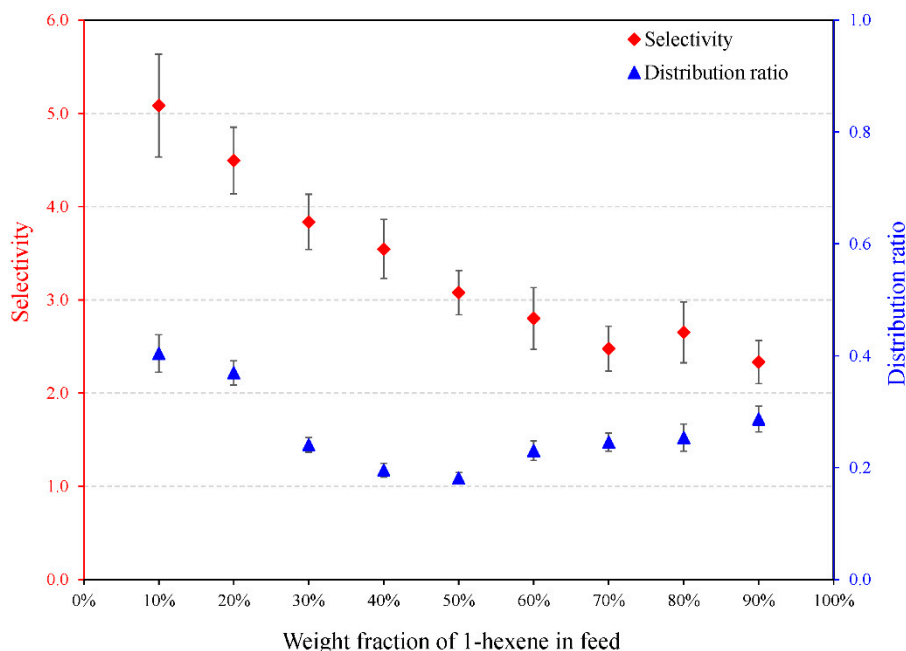
Figure 7. Variation of the selectivity and the distribution ratio with toluene weight fraction in the feed for {1-hexene (1) + toluene (2) + DES #3 (3)}.

4.2. Consistency Test

The Othmer–Tobias and Hand correlations were applied to perform the consistency tests of the experimental data. The correlations that were used to express the Othmer–Tobias [28] and Hand [29] equations, respectively, are given below:

$$ ln\left(\frac{1 - w''_{hex}}{w''_{hex}}\right) = a + b \, ln\left(\frac{1 - w'_{DES}}{w'_{DES}}\right) \tag{7} $$

$$ ln\left(\frac{w''_{tol}}{w''_{hex}}\right) = c + d \, ln\left(\frac{w'_{tol}}{w'_{DES}}\right) \tag{8} $$

In the above equations, w_{hex}, w_{DES}, and w_{tol} refer to the concentrations of 1-hexene DES, and toluene, respectively. *a* and *b* denote the fitting parameters of the Othmer–Tobias correlation, while *c* and *d* are the fitting parameters of the Hand correlation. The superscripts $'$ and $''$ denote the bottom and top layers, respectively. The parameters of the Othmer–Tobias and Hand equations are listed in Table 9. The linearity of the plot (the regression coefficient R^2 is close to 1) indicates the degree of consistency of the experimental data.

Table 9. Othmer–Tobias and Hand correlations parameters.

DES	Othmer–Tobias			Hand		
	a	b	R^2	c	d	R^2
DES #1	3.468	1.859	0.964	2.951	1.336	0.966
DES #2	2.619	1.109	0.953	2.357	0.883	0.956
DES #3	5.490	2.189	0.940	5.444	1.847	0.963

4.3. Comparison between DESs and Organic Solvents

Various organic solvents were used for the extraction of toluene from n-haptane (Table S12). Among the organic solvents, TEG showed higher selectivity than other organic solvents [30]. While ethylene glycol (EG) showed the lowest distribution ratio [31]. Sulfolane showed good results in both selectivity and the distribution ratio in the extraction of toluene from n-heptane [32]. For this reason, sulfolane is usually used as a benchmark for evaluating the performance of other solvents. In Table S2, the performance of organic solvents was also compared with ILs.

The selectivity of 1-ethyl-3-methylimidazolium thiocyanate ([emim][SCN]) and 1-butyl-3-methylimidazolium thiocyanate ([bmim][SCN]) ILs was higher than that of organic solvents [33]. Dukhande [34] reported the use of monocationic and dicationic ILs for the separation of toluene/heptane. The dicationic ILs showed a slightly higher distribution ratio and selectivity compared to the monocationic ILs. This result was attributed to the increasing interaction between IL and toluene in the raffinate. González et al. [35] reported the extraction of toluene from various aliphatic compounds, including hexane, heptane, octane and nonane, using 1-ethyl-3-methylimidazolium ethyl sulphate ([EMim][ESO4]) as solvent. It was found that increasing the chain length of alkane resulted in increased value of selectivity in the order hexane < heptane < octane < nonane. On the other hand, the chain length of alkane showed a weak effect on the distribution ratio, as almost all values were in the range of 0.20–0.28.

Liquid–liquid experiments with the three DESs studied in this work and two other common organic solvents, including sulfolane and triethylene glycol, were performed for the separation of the binary mixture toluene/1-hexene at 50 wt%. The results obtained are listed in Table 10. All DESs depicted a higher performance index than organic solvents.

Table 10. Composition of the experimental tie-lines (mole fraction), the toluene distribution ratio (D), selectivity (S), and the performance index (PI) for the ternary system {1-hexene (1) + toluene (2) + solvent (3)} at 298.15 K and 101.325 kPa.

Top Layer			Bottom Layer			D_{tol}	S	PI
x_1	x_2	x_3	x_1	x_2	x_3			
			Sulfolane					
0.591 ± 0.02	0.409 ± 0.014	0	0.057 ± 0.001	0.162 ± 0.004	0.781 ± 0.020	0.397 ± 0.006	4.13 ± 0.35	1.640
			Triethylene glycol					
0.582 ± 0.021	0.418 ± 0.015	0	0.058 ± 0.002	0.151 ± 0.040	0.791 ± 0.021	0.361 ± 0.003	3.66 ± 0.26	1.321

Table 10. *Cont.*

Top Layer			Bottom Layer			D_{tol}	S	PI
x_1	x_2	x_3	x_1	x_2	x_3			
			[3-mebupy]N(CN)$_2$ [a]					
0.6180	0.3795	0	0.0192	0.1059	0.8749	0.279	9.0	2.511
			DES #1					
0.568 ± 0.021	0.432 ± 0.016	0	0.052 ± 0.003	0.180 ± 0.007	0.769 ± 0.029	0.416 ± 0.007	4.55 ± 0.50	1.893
			DES #2					
0.551 ± 0.021	0.449 ± 0.017	0	0.095 ± 0.004	0.370 ± 0.010	0.535 ± 0.020	0.822 ± 0.005	4.78 ± 0.51	3.929
			DES #3					
0.541 ± 0.021	0.459 ± 0.018	0	0.109 ± 0.002	0.285 ± 0.050	0.606 ± 0.031	0.621 ± 0.002	3.08 ± 0.33	1.913

[a] Data are taken from [3] at T = 303.15 K.

The relatively low values of selectivity and the distribution ratio obtained with all the solvents confirm the difficulty of such separation and the fact that the three DESs studied in this work can compete with traditional organic solvents.

4.4. NRTL Correlation

When designing or simulating industrial processes, it is important to have a reliable thermodynamic model that can accurately describe the phase behavior of pure compounds and their mixtures over a wide range of operating conditions. The non-random two-liquid model (NRTL) is one such model widely used to describe the non-ideality of the liquid phase of various systems, including ionic liquids and deep eutectic solvents. This model was used here to regress the previously reported experimental LLE data (Tables 6–8). The model was developed in the Simulis® Thermodynamics environment, a server for calculating thermophysical properties provided by ProSim company [36]. Phase compositions in liquid–liquid equilibrium were calculated by solving the isothermal liquid–liquid flash at a given pressure and temperature, represented by these equations:

$$\text{Material balance}: \qquad x_i - (1 - \omega)x_i^I - \omega x_i^{II} = 0 \qquad i = 1, \ N_C \qquad (9)$$

$$\text{Equilibrium equation}: \qquad x_i^I \gamma_i^I - x_i^{II} \gamma_i^{II} = 0 \qquad i = 1, \ N_C \qquad (10)$$

$$\text{Equation of summation}: \qquad \sum x_i^I - \sum x_i^{II} = 0 \qquad (11)$$

where, x_i is the composition of component i in the mixture, x_i^j is the composition of component i in the liquid phase j, ω is the liquid–liquid splitting ratio, γ_i^j is the activity coefficient of component i in the liquid phase j, and N_C is the number of constituents.

For a multi-component system, the activity coefficient is described in the NRTL model by the following equation [37]:

$$n\gamma_i = \frac{\sum_j \tau_{ji} G_{ji} x_j}{\sum_j G_{ji} x_j} + \sum_j \frac{G_{ij} x_j}{\sum_k G_{kj} x_k} \left(\tau_{ij} - \frac{\sum_k \tau_{kj} G_{kj} x_k}{\sum_k G_{kj} x_k} \right) \qquad (12)$$

with $lnG_{ij} = -\alpha_{ij}\tau_{ij}$; $\alpha_{ij} = \alpha_{ji}$; $\tau_{ij} = \frac{g_{ij} - g_{ii}}{RT} = \frac{C_{ij}}{RT}$; $\tau_{ii} = \tau_{jj} = 0$, where τ_{ij} and τ_{ji} are the binary interaction parameters and α_{ij} is the non-randomness parameter.

In this work, we set the non-randomness parameter α_{ij} constant to 0.20 for all binary combinations as it previously gave an exact fit for ternary LLE systems involving DESs [38,39]. Then, the binary interaction parameters C_{ij}, C_{ji} at 298.15 K were estimated by minimizing the root mean square deviation (RMSD) between the calculated and experimental compositions in each phase:

$$RMSD \ (\%) = 100 \sqrt{\sum_{k=1}^{m} \sum_{i=1}^{c} \sum_{j=1}^{2} \frac{\left(x_{ik}^{j} - \hat{x}_{ik}^{j}\right)^{2}}{2mc}} \tag{13}$$

where x is the concentration of species in a mole fraction, and subscripts i, j, and k designate the component, phase, and tie line, respectively. In addition, m is the number of tie-lines, c is the number of components, and j refers to the phases.

Table 11 lists the values of the binary interaction parameters obtained using the NRTL model with each ternary system. To minimize the number of regression parameters and to ensure some coherence, the interaction between 1-hexene and toluene was considered independent of DES. The calculated and experimental tie-lines agree well, with RMSD not exceeding 2%. The calculated tie-lines can be found in the supporting material (Tables S13–S15) and are represented by dashed lines in the ternary diagrams (Figure 4).

Table 11. NRTL interaction parameters for each ternary system with the corresponding RMSD.

i–j	τ_{ij}	τ_{ji}
1-hexene–Toluene	−102.6	−518.1
	RMSD for DES #1 = 1.75%	
1-hexene–DES #1	1385.3	246.8
Toluene–DES #1	2737.4	−344.5
	RMSD for DES #2 = 1.30%	
1-hexene–DES #2	1615.8	621.9
Toluene–DES #2	1697.9	−392.4
	RMSD for DES #3 = 1.58%	
1-hexene–DES #3	1389.8	194.3
Toluene–DES #3	2700.8	−74.3

5. Conclusions

The separation of aromatics from aromatic and olefin mixtures is an exciting challenge for the chemical and petrochemical industry and many types of solvents have been studied for this purpose, including classical organic solvents, ionic liquids or deep eutectic solvents. In this work, we experimentally studied three DESs, namely BzTPPCl:TEG (1:8), TBABr:TEG (1:3) and TBABr:EG (1:4), as potential extractants for the separation of the binary system {1-hexene + toluene}. These DESs were selected from more than 50 potential candidates based on a preliminary COSMO-RS screening study by predicting the activity coefficient at infinite dilution. Among all the DESs tested, TBABr:TEG (1:3) showed the relatively best performance in terms of both selectivity and the distribution ratio. The experimental LLE data were measured for the ternary systems at T = 298.15 K and atmospheric pressure. Moreover, minimal cross-contamination was found between the extract and raffinate phases, as no DES was found in the raffinate phase. Furthermore, the results show that the DESs studied here can compete with the conventional organic solvents usually used for such separation.

Tables S7 and S8: Standard deviation STDEV on measured solubilities of 1-hexene (1)/toluene (2) mixture with DES #3 (3) for mole fractions x: Top layer and bottom layer. Tables S9–S11: GC data of top and bottom layers for 1-hexene (1)/toluene (2) mixture with DES #i (3). Table S12: Summary of performance extraction of toluene/heptane using organic solvents and ILs. Tables S13–S15: Composition of the NRTL tie-lines (mole fraction), for the ternary system {1-hexene (1) + toluene (2) + DES #i (3)} at 298.15 K and 101.325 kPa. References [12–14,30–35,40] are cited in the supplementary materials.

Author Contributions: Conceptualization, M.K.H.-K., J.R. and E.A.; methodology, M.K.H.-K. and L.E.B.; software, M.K.H.-K.; validation, I.W., L.E.B. and S.M.; formal analysis, L.E.B., I.W. and S.M.; investigation, M.K.H.-K.; resources, L.E.B., I.W. and S.M.; data curation, M.K.H.-K., J.R. and E.A.; writing—original draft preparation, M.K.H.-K. and I.W.; writing—review and editing, M.K.H.-K., I.W. and E.A.; visualization, L.E.B., J.R. and S.M.; supervision, M.K.H.-K. and E.A.; project administration, M.K.H.-K., J.R. and E.A.; funding acquisition, M.K.H.-K. and J.R. All authors have read and agreed to the published version of the manuscript.

Institutional Review Board Statement: Not applicable.

Informed Consent Statement: Not applicable.

Data Availability Statement: Not applicable.

Appendix A

The uncertainty of weighing was included in all calculation using following equation:

$$u_{cBAL}(\%) = \sqrt{r_{BAL}^2 + \sigma_{BAL}^2}$$

where: random component (r_{BAL}): $r_{BAL}^2 = \frac{S.D._w}{m_A} \times 100$

$S.D._w$ is standard deviation of repeated weighing of empty vial (V = 10 mL).

The systematic component (σ_{BAL}) of uncertainty of weighing was calculated for each compound according to: $\sigma_{BAL}^2 = \frac{a}{m_A \times \sqrt{3}} \times 100$

Analytical balance uncertainty or weighing tolerance ($\pm$0.1 mg).

Appendix A.1 Uncertainty Calculations for LLE Data

For the calculation of different compositions, we have considered the uncertainties associated with GC analysis, uncertainties of weighing, diluting of hydrocarbons, and uncertainties of purity of all chemicals used in this work [41].

Combined uncertainties were used for calculation of combined standard uncertainty u_c associated with analytical method employed for hydrocarbons analysis—see Equation below:

$$u_c(\%) = \sqrt{u_{cGC}^2 + u_{cBAL}^2 + u_{cDIL}^2 + u_{cSTD}^2}$$

where: u_{cGC} represents combined uncertainty of GC step, $u_{cGC}(\%) = \sqrt{r_{GC}^2 + u(R)_{GC}^2}$

r are repeatabilities (uncertainties type A, random errors) obtained from GC analysis.

$u(R)$ is uncertainty of recovery (uncertainties type B, systematic errors) obtained from GC analysis.

u_{cBAL} represents combined uncertainty of weighing, $u_{cBAL}(\%) = \sqrt{r_{BAL}^2 + \sigma_{BAL}^2}$

Uncertainty of weighing. The random component (r_{BAL}) of this operation was calculated using: $r_{BAL}^2 = \frac{S.D._w}{m_A} \times 100$

Where $S.D._w$ is standard deviation of repeated weighing of empty vial (V = 10 mL) which was used for LLE tests and m_A is the amount of hydrocarbons used for the prepa-

ration of DESs and LLE experiments. The systematic component (σ_{BAL}) of uncertainty of weighing was calculated for each compound according to: $\sigma_{BAL}^2 = \frac{a}{m_A \times \sqrt{3}} \times 100$

Where a is a weighing tolerance declared in the calibration certificate of balances (± 0.1 mg).

u_{cDIL} represents combined uncertainty of dilution. $u_{cDIL}(\%) = \sqrt{r_{DIL}^2 + \sigma_{DIL}^2}$

Uncertainty of dilution. The random component (r_{BAL}) of this operation was calculated using: $r_{DIL}^2 = \frac{S.D._B}{m_B} \times 100$

Where $S.D._B$ is standard deviation of repeated weighing of known volume measured by the micropipette (V = 1000 µL) which was used for LLE tests and m_B is the amount of hydrocarbons used for the preparation of DESs and LLE experiments. The systematic component (σ_{DIL}) of The confidence interval $\pm$b of a micropipette supplied by manufacturer (± 1.5 µL) was used for calculating the systematic component of uncertainty (σ_{DIL}): $\sigma_{DIL}^2 = \frac{b}{V \times \sqrt{3}} \times 100$

u_{cSTD}, Uncertainty of purity of hydrocarbons. $u_{cSTD}(\%) = \frac{0.5 \times (100 - y)}{\sqrt{3}}$

Where $y(\%)$ represents the purity of hydrocarbons and DES constituents given in the manufacturer specification

Since we have used GC data for composition calculation, the errors uncertainties of areas were propagated to all calculation.

Each GC analysis was triplicated and the systematic uncertainty was used to calculate the average value and the error certainty related to this value.

Appendix A.2 Uncertainty Calculations for Selectivity and Distribution Ratio

To determine uncertainties for *S* and *D*, we have included uncertainties from *GC* analysis and systematic errors obtained by triplicating analysis:

The uncertainties were first calculated for areas of GC analysis:

$$u_c(\%) = \sqrt{u_{cGC}^2 + u_{cBAL}^2 + u_{cDIL}^2 + u_{cSTD}^2}$$

The composition was calculated from the relation between *GC* areas and composition as mole number (*n*) using calibration curve. Two uncertainties were considered: systematic uncertainty (triplicates) and relative uncertainty:

$$u_n(\%) = \sqrt{u_{hexGC}^2 + u_{tolGC}^2 + u_{cBAL}^2 + u_{cDIL}^2 + u_{cSTD}^2}$$

After determination of number of moles of each components, the composition was calculated for each component and for both phases:

$$u_{x(hex)}(\%) = \sqrt{u_{n(hex)}^2 + u_{n(tol)}^2 + u_{n(DES)}^2}$$

References

1. Liu, J.; Liu, N.; Ren, K.; Shi, L.; Meng, X. Sulfated zirconia synthesized in a one step solvent-free method for removal of olefins from aromatics. *Ind. Eng. Chem. Res.* **2017**, *56*, 7693–7699. [CrossRef]
2. Coquelet, C.; Ramjugernath, D. Phase Diagrams in Chemical Engineering: Application to Distillation and Solvent Extraction. In *Advances in Chemical Engineering*; IntechOpen: London, UK, 2012; pp. 483–504.
3. Meindersma, W.; Onink, F.; Hansmeier, A.R.; de Haan, A.B. Long term pilot plant experience on aromatics extraction with ionic liquids. *Sep. Sci. Technol.* **2012**, *47*, 337–345. [CrossRef]
4. Kareem, M.A.; Mjalli, F.S.; Hashim, M.A.; AlNashef, I.M. Liquid–liquid equilibria for the ternary system (phosphonium based deep eutectic solvent–benzene–hexane) at different temperatures: A new solvent introduced. *Fluid Phase Equilib.* **2012**, *314*, 52–59. [CrossRef]
5. Wang, Y.; Hou, Y.; Wu, W.; Liu, D.; Ji, Y.; Ren, S. Roles of a hydrogen bond donor and a hydrogen bond acceptor in the extraction of toluene from n-heptane using deep eutectic solvents. *Green Chem.* **2016**, *18*, 3089–3097. [CrossRef]
6. Hou, Y.; Li, Z.; Ren, S.; Wu, W. Separation of toluene from toluene/alkane mixtures with phosphonium salt based deep eutectic solvents. *Fuel Process. Technol.* **2015**, *135*, 99–104. [CrossRef]

7.　Petkovic, M.; Seddon, K.R.; Rebelo, L.P.N.; Pereira, C.S. Ionic liquids: A pathway to environmental acceptability. *Chem. Soc. Rev.* **2011**, *40*, 1383–1403. [CrossRef]

8.　Steudte, S.; Stepnowski, P.; Cho, C.-W.; Thöming, J.; Stolte, S. (Eco) toxicity of fluoro-organic and cyano-based ionic liquid anions. *Chem. Commun.* **2012**, *48*, 9382–9384. [CrossRef]

9.　Wazeer, I.; Hayyan, M.; Hadj-Kali, M.K. Deep eutectic solvents: Designer fluids for chemical processes. *J. Chem. Technol. Biotechnol.* **2018**, *93*, 945–958. [CrossRef]

10.　Yu, Y.; Lu, X.; Zhou, Q.; Dong, K.; Yao, H.; Zhang, S. Biodegradable naphthenic acid ionic liquids: Synthesis, characterization, and quantitative structure–biodegradation relationship. *Chem. A Eur. J.* **2008**, *14*, 11174–11182. [CrossRef]

11.　Hayyan, M.; Hashim, M.A.; Hayyan, A.; Al-Saadi, M.A.; AlNashef, I.M.; Mirghani, M.E.; Saheed, O.K. Are deep eutectic solvents benign or toxic? *Chemosphere* **2013**, *90*, 2193–2195. [CrossRef]

12.　Naik, P.K.; Dehury, P.; Paul, S.; Banerjee, T. Evaluation of Deep Eutectic Solvent for the selective extraction of toluene and quinoline at T = 308.15 K and p = 1 bar. *Fluid Phase Equilib.* **2016**, *423*, 146–155. [CrossRef]

13.　Gouveia, A.S.; Oliveira, F.S.; Kurnia, K.A.; Marrucho, I.M. Deep eutectic solvents as azeotrope breakers: Liquid–liquid extraction and COSMO-RS prediction. *ACS Sustain. Chem. Eng.* **2016**, *4*, 5640–5650. [CrossRef]

14.　Kareem, M.A.; Mjalli, F.S.; Hashim, M.A.; Hadj-Kali, M.K.; Bagh, F.S.G.; Alnashef, I.M. Phase equilibria of toluene/heptane with deep eutectic solvents based on ethyltriphenylphosphonium iodide for the potential use in the separation of aromatics from naphtha. *J. Chem. Thermodyn.* **2013**, *65*, 138–149. [CrossRef]

15.　Anantharaj, R.; Banerjee, T. Aromatic sulfur-nitrogen extraction using ionic liquids: Experiments and predictions using an a priori model. *AIChE J.* **2013**, *59*, 4806–4815. [CrossRef]

16.　Anantharaj, R.; Banerjee, T. COSMO-RS based predictions for the desulphurization of diesel oil using ionic liquids: Effect of cation and anion combination. *Fuel Process. Technol.* **2011**, *92*, 39–52. [CrossRef]

17.　Wilfred, C.D.; Man, Z.; Chan, Z.P. Predicting methods for sulfur removal from model oils using COSMO-RS and partition coefficient. *Chem. Eng. Sci.* **2013**, *102*, 373–377. [CrossRef]

18.　Zhou, T.; Wang, Z.; Ye, Y.; Chen, L.; Xu, J.; Qi, Z. Deep separation of benzene from cyclohexane by liquid extraction using ionic liquids as the solvent. *Ind. Eng. Chem. Res.* **2012**, *51*, 5559–5564. [CrossRef]

19.　Gonfa, G.; Bustam, M.A.; Murugesan, T.; Man, Z.; Mutalib, M. Thiocyanate based task-specific ionic liquids for separation of benzene and cyclohexane. *Chem. Eng.* **2013**, *32*, 1939–1944.

20.　Lyu, Z.; Zhou, T.; Chen, L.; Ye, Y.; Sundmacher, K.; Qi, Z. Simulation based ionic liquid screening for benzene–cyclohexane extractive separation. *Chem. Eng. Sci.* **2014**, *113*, 45–53. [CrossRef]

21.　Mulyono, S.; Hizaddin, H.F.; Wazeer, I.; Alqusair, O.; Ali, E.; Hashim, M.A.; Hadj-Kali, M.K. Liquid-liquid equilibria data for the separation of ethylbenzene/styrene mixtures using ammonium-based deep eutectic solvents. *J. Chem. Thermodyn.* **2019**, *135*, 296–304. [CrossRef]

22.　Wazeer, I.; Hizaddin, H.F.; El Blidi, L.; Ali, E.; Hashim, M.A.; Hadj-Kali, M.K. Liquid–Liquid Equilibria for Binary Azeotrope Mixtures of Benzene and Alcohols Using Choline Chloride-Based Deep Eutectic Solvents. *J. Chem. Eng. Data* **2018**, *63*, 613–624. [CrossRef]

23.　Salleh, Z.; Hadj-Kali, M.; Hashim, M.A.; Mulyono, S. Ionic liquids for the separation of benzene and cyclohexane—COSMO-RS screening and experimental validation. *J. Mol. Liq.* **2018**, *266*, 51–61. [CrossRef]

24.　Salleh, Z.; Wazeer, I.; Mulyono, S.; El-blidi, L.; Hashim, M.A.; Hadj-Kali, M. Efficient removal of benzene from cyclohexane-benzene mixtures using deep eutectic solvents—COSMO-RS screening and experimental validation. *J. Chem. Thermodyn.* **2017**, *104*, 33–44. [CrossRef]

25.　Abbott, A.P.; Boothby, D.; Capper, G.; Davies, D.L.; Rasheed, R.K. Deep eutectic solvents formed between choline chloride and carboxylic acids: Versatile alternatives to ionic liquids. *J. Am. Chem. Soc.* **2004**, *126*, 9142–9147. [CrossRef] [PubMed]

26.　Chirico, R.D.; Frenkel, M.; Magee, J.W.; Diky, V.; Muzny, C.D.; Kazakov, A.F.; Kroenlein, K.; Abdulagatov, I.; Hardin, G.R.; Acree, W.E., Jr. Improvement of quality in publication of experimental thermophysical property data: Challenges, assessment tools, global implementation, and online support. *J. Chem. Eng. Data* **2013**, *58*, 2699–2716. [CrossRef]

27.　Taylor, B.N.; Kuyatt, C.E. *Guidelines for Evaluating and Expressing the Uncertainty of NIST Measurement Results*; US Department of Commerce, Technology Administration, National Institute of Standards and Technology: Gaithersburg, MD, USA, 1994; Volume 1297.

28.　Othmer, D.; Tobias, P. Liquid-liquid extraction data-the line correlation. *Ind. Eng. Chem.* **1942**, *34*, 693–696. [CrossRef]

29.　Hand, D.B. Dineric Distribution. *J. Phys. Chem.* **1929**, *34*, 1961–2000. [CrossRef]

30.　Salem, A.B.S. Liquid-liquid equilibria for the systems triethylene glycol-toluene-heptane, propylene carbonate-toluene-heptane and propylene carbonate-o-xylene-heptane. *Fluid Phase Equilib.* **1993**, *86*, 351–361. [CrossRef]

31.　Haghnazarloo, H.; Lotfollahi, M.N.; Mahmoudi, J.; Asl, A.H. Liquid–liquid equilibria for ternary systems of (ethylene glycol+ toluene+ heptane) at temperatures (303.15, 308.15, and 313.15) K and atmospheric pressure: Experimental results and correlation with UNIQUAC and NRTL models. *J. Chem. Thermodyn.* **2013**, *60*, 126–131. [CrossRef]

32.　Hassan, M.S.; Fahim, M.A.; Mumford, C.J. Correlation of phase equilibria of naphtha reformate with sulfolane. *J. Chem. Eng. Data* **1988**, *33*, 162–165. [CrossRef]

33.　Larriba, M.; Navarro, P.; García, J.; Rodríguez, F. Selective extraction of toluene from n-heptane using [emim][SCN] and [bmim][SCN] ionic liquids as solvents. *J. Chem. Thermodyn.* **2014**, *79*, 266–271. [CrossRef]

34. Dukhande, V.A.; Choksi, T.S.; Sabnis, S.U.; Patwardhan, A.W.; Patwardhan, A.V. Separation of toluene from n-heptane using monocationic and dicationic ionic liquids. *Fluid Phase Equilib.* **2013**, *342*, 75–81. [CrossRef]

35. González, E.J.; Calvar, N.; Domínguez, I.; Domínguez, Á. Extraction of toluene from aliphatic compounds using an ionic liquid as solvent: Influence of the alkane on the (liquid+ liquid) equilibrium. *J. Chem. Thermodyn.* **2011**, *43*, 562–568. [CrossRef]

36. Simulis®, Thermodynamics. Available online: http://www.Prosim.Net (accessed on 22 October 2022).

37. Renon, H.; Prausnitz, J.M. Local compositions in thermodynamic excess functions for liquid mixtures. *AIChE J.* **1968**, *14*, 135–144. [CrossRef]

38. Mulyono, S.; Hizaddin, H.F.; Alnashef, I.M.; Hashim, M.A.; Fakeeha, A.H.; Hadj-Kali, M.K. Separation of BTEX aromatics from n-octane using a (tetrabutylammonium bromide+ sulfolane) deep eutectic solvent–experiments and COSMO-RS prediction. *RSC Adv.* **2014**, *4*, 17597–17606. [CrossRef]

39. Hizaddin, H.F.; Sarwono, M.; Hashim, M.A.; Alnashef, I.M.; Hadj-Kali, M.K. Coupling the capabilities of different complexing agents into deep eutectic solvents to enhance the separation of aromatics from aliphatics. *J. Chem. Thermodyn.* **2015**, *84*, 67–75. [CrossRef]

40. Mohsen-Nia, M.; Doulabi, F.M. Separation of aromatic hydrocarbons (toluene or benzene) from aliphatic hydrocarbon (n-heptane) by extraction with ethylene carbonate. *J. Chem. Thermodyn.* **2010**, *42*, 1281–1285. [CrossRef]

41. Štěpán, R.; Hajšlová, J.; Kocourek, V.; Tichá, J. Uncertainties of gas chromatographic measurement of troublesome pesticide residues in apples employing conventional and mass spectrometric detectors. *Anal. Chim. Acta* **2004**, *520*, 245–255. [CrossRef]